Available online at www.sciencedirect.com
SCIENCE DIRECT
Journal of Power Sources 119–121 (2003) 870–873
JOURNAL OF POWER SOURCES
www.elsevier.com/locate/jpowsour

Accelerated calendar and pulse life analysis of lithium-ion cells

Rudolph G. Jungst*, Ganesan Nagasubramanian, Herbert L. Case, Bor Yann Liaw, Angel Urbina, Thomas L. Paez, Daniel H. Doughty

Sandia National Laboratories, Albuquerque, NM 87185, USA

Abstract

Sandia National Laboratories has been studying calendar and pulse discharge life of prototype high-power lithium-ion cells as part of the Advanced Technology Development (ATD) Program. One of the goals of ATD is to establish validated accelerated life test protocols for lithium-ion cells in the hybrid electric vehicle application. In order to accomplish this, aging experiments have been conducted on 18650-size cells containing a chemistry representative of these high-power designs. Loss of power and capacity are accompanied by increasing interfacial impedance at the cathode. These relationships are consistent within a given state-of-charge (SOC) over the range of storage temperatures and times. Inductive models have been used to construct detailed descriptions of the relationships between power fade and aging time and to relate power fade, capacity loss and impedance rise. These models can interpolate among the different experimental conditions and can also describe the error surface when fitting life prediction models to the data.
Published by Elsevier Science B.V.

Keywords: Lithium-ion cell; Inductive modeling; Artificial neural networks

1. Introduction

The Advanced Technology Development (ATD) Program is sponsored by the US Department of Energy, to support the development of high-power battery systems for use in hybrid electric vehicles (HEV). Goals of the ATD Program include determining causes for power fade in lithium-ion batteries and predicting HEV battery life, developing analytical tools that can be used to measure battery degradation and identify failure mechanisms, identifying causes for intolerance to thermal abuse and improving battery safety, and reducing the cost of battery materials and fabrication processes. This paper discusses the continued development of advanced computational tools for predicting battery life in a variety of environments and use profiles [1]. General methods are desired that can be applied to different sources and types of vehicle batteries. In the long term, these results will be correlated with quantitative diagnostic measurements of degradation mechanisms to validate that mechanisms do not change at increased levels of acceleration or at longer times. The mechanistic approach may also offer the possibility of higher sensitivity so that degradation can be detected earlier in the aging process. However, this report concentrates on results from an empirical approach that forces measurable change in cell performance. In particular, the ability of inductive models to efficiently interpolate and predict cell performance for conditions that were not tested and to model error surfaces for cell performance prediction models were investigated.

2. Experiments and aging results

An 18650-size Li-ion cell is being used by the ATD program to investigate power fade at various experimental conditions of temperature, state-of-charge (SOC) and pulse discharge profile. These cells contain no internal safety components such as positive temperature coefficient (PTC) devices that could limit cell performance. Representative high-power cell chemistry was used, consisting of a MAG-10 graphite negative electrode, a $LiNi_{0.8}Co_{0.15}Al_{0.05}O_2$ positive electrode, poly(vinylidine difluoride) binder, and a 1.2 M $LiPF_6$ in ethyl carbonate/ethyl methyl carbonate (3:7 wt.% ratio) electrolyte.

Initial experiments have focused on the parameters of temperature and SOC in a calendar-aging test. The test profile includes a single daily discharge to track increases in cell resistance, but otherwise the samples are stored at a controlled voltage corresponding to the desired SOC. Reduction of these test data to power fade metrics has been described in previous publications [2,3]. Experiments were

* Corresponding author. Tel.: +1-505-844-1103; fax: +1-505-844-6972.
E-mail address: rgjungs@sandia.gov (R.G. Jungst).

0378-7753/03/$ – see front matter. Published by Elsevier Science B.V.
doi:10.1016/S0378-7753(03)00193-9

carried out at temperatures of 25, 35, 45, or 55 °C and at 60, 80, or 100% SOC in order to force cells to degrade rapidly so that degradation rates could be determined. Data available through 24 weeks of aging show that both power capability and capacity decrease. The experiment plan was designed for statistical analysis and includes at least three replicates at each set of conditions. Parameter values cover the expected range in HEV use, which allows extrapolation of measured accelerated power fade rates to the nominal use condition (25 °C and 60% SOC) to be validated. Use of a minimum of three levels for each of the parameters also enables nonlinear effects and interactions between the parameters to be assessed.

3. Correlation of power fade with electrochemical impedance spectroscopy

In addition to measuring loss of power capability and capacity after every 4-week aging interval, electrochemical impedance spectroscopy (EIS) measurements were also made at two states of charge during each of these reference performance test (RPT) evaluations. NyQuist plots of the EIS data show a single major interfacial impedance loop for these cells after aging as shown in Fig. 1. There is continual growth in the width of this loop with time that is most apparent at high temperature. Aging at 100% SOC also causes greater interfacial impedance. As can be seen in Fig. 1, all other contributions to the impedance (e.g. the ohmic impedance or zero crossing point and the diffusion region at low frequency) remain relatively constant during aging. The dominant interfacial EIS component has been assigned to the cathode in this lithium-ion cell chemistry through use of three-electrode studies [4]. Since only the interfacial impedance is changing while power fade is occurring, it was of interest to see whether there was a consistent correlation with the power

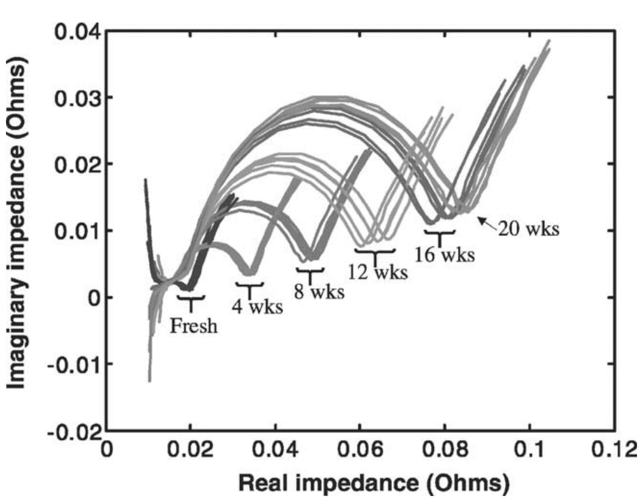

Fig. 1. Li-ion cell impedance data at 100% SOC after aging at 100% SOC, 55 °C.

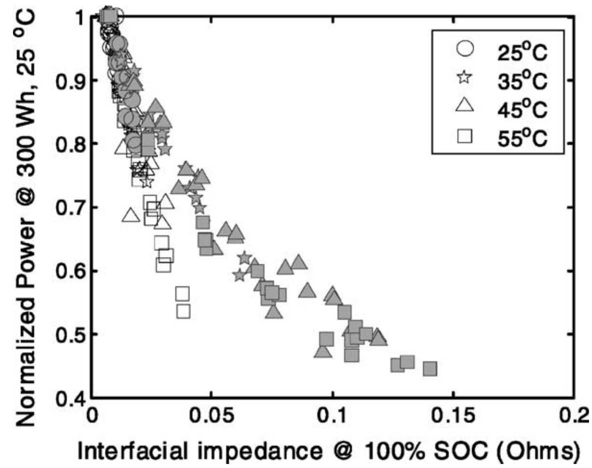

Fig. 2. Correlation of Li-ion cell power capability with interfacial impedance (filled markers represent aging at 100% SOC and unfilled markers represent aging at 60% SOC).

measurements. Fig. 2 shows that there is a correlation between these two parameters, but that the nature of the correlation is different for each SOC during aging. There is a particularly large difference between the 100% SOC correlation and the 60% SOC correlation. The cause for this has not been determined at present, but is under investigation.

4. Artificial neural network modeling approach

Artificial neural networks (ANN) are frameworks for creating inductive mappings and we use them to model the input/output relations in lithium-ion electrochemical cells. The output is a measure of power fade in lithium-ion cells while cell capacity, aging time, state of charge and various metrics of cell impedance are used as inputs to the ANN. The ANN used here is the multivariate linear spline (MVLS) network which is a generalization of the connectionist normalized linear spline (CNLS) network [5] to multiple input/output dimensions. The MVLS network, written in Matlab and developed at Sandia is well suited to this application due to its ability to model complex, nonlinear relationships. The following is a brief description of the MVLS network; a more detailed explanation can found in [6].

To commence, we let $\boldsymbol{x}$ be an n-dimensional input vector to the system being modeled, and let $z = g(\boldsymbol{x})$ be its corresponding m-dimensional output vector. We assume that the function $g(\boldsymbol{x})$ is deterministic but that its form and parameters are unknown. We can approximate the mapping from $\boldsymbol{x}$ to z in a region of the input/output space using the linear form:

$$z \cong \boldsymbol{y} = \boldsymbol{A}(\boldsymbol{x} - \boldsymbol{c}) \tag{1}$$

where $\boldsymbol{y}$ is an approximation to z, $\boldsymbol{c}$ a vector with the same dimension as $\boldsymbol{x}$ in the vicinity of which the approximation is made, and $\boldsymbol{A}$ a matrix of constants. This approximation needs to be optimized using least squares or weighted least squares and is accurate in the vicinity of the data used to develop it as long as the behavior of the mapping in the neighborhood is truly linear. The vector $\boldsymbol{c}$ is the ''center'' of the local linear approximation. We can develop similar approximations in other neighborhoods of the input vector space. Having developed local linear approximations of the $\boldsymbol{x}$ to z mapping, we can now combine the local approximations to create an approximate, global map. The approximation takes an input vector $\boldsymbol{x}_0$ and maps into $\boldsymbol{y}_0$, an approximation to $g(\boldsymbol{x}_0)$. To accomplish this, we superimpose several of the linear approximations in a series. We weight each component in the series according to its distance from the input vector $\boldsymbol{x}_0$. Local linear models that are near $\boldsymbol{x}_0$ are weighted heavily, whereas those that are further away are weighted less. The series is:

$$\sum_j \boldsymbol{y}_0 \boldsymbol{w}_j = \sum_j \boldsymbol{A}_j(\boldsymbol{x}_0 - \boldsymbol{c}_j)\boldsymbol{w}_j \tag{2}$$

where the $\boldsymbol{w}_j$ are the weights attached to the local linear models. The output vector $\boldsymbol{y}_0$ on the left side is independent of the index j, so it can be removed from the sum, and the equation can be simplified to:

$$\boldsymbol{y}_0 = \frac{\sum_j \boldsymbol{A}_j(\boldsymbol{x}_0 - \boldsymbol{c}_j)\boldsymbol{w}_j}{\sum_j \boldsymbol{w}_j} \tag{3}$$

This is the parametric form of the MVLS network and we choose the form of the multivariate Gaussian probability density function (also known as a radial basis function) for the weighting expression. The MVLS network is used in the feed forward operation by specifying the input vector $\boldsymbol{x}_0$, evaluating the weights $\boldsymbol{w}_j$, substituting the weights and input vector into Eq. (3), and evaluating the output $\boldsymbol{y}_0$. This output should present an interpolation among the training outputs that corresponds to the input as an interpolation among the training inputs.

5. Experimental/numerical examples

Several numerical examples of the use of these tools to predict power fade of lithium-ion cells are presented in this section. We have trained different ANNs to simulate the input/output characteristics of some lithium-ion cell measures of behavior. The first case looks at the relationship between aging time, SOC and a metric of the power fade measured at 25 °C. Aging time is represented by the RPT number, which is defined as the periodic evaluation of cell performance at 4-week intervals during aging. Fig. 3 shows the ANN map of these variables for cells aged at 55 °C. The dots represent the experimental data and the surface was calculated using the ANN fit to this data. Interpolation and very limited extrapolation were done. The ANN clearly captures the trend of the data, which indicates a decrease

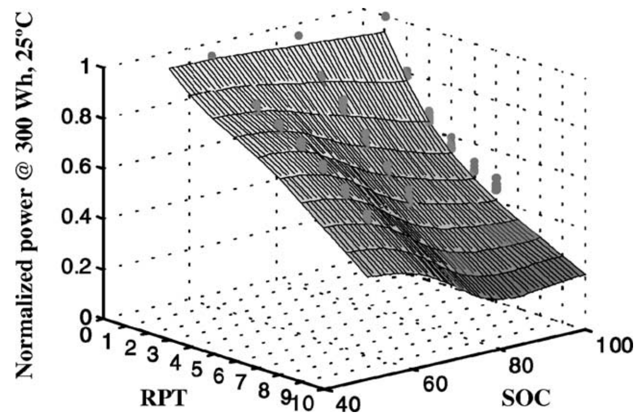

Fig. 3. ANN map of aging time (RPT#), SOC and a metric of power fade.

in power capability as aging occurs, and at higher states of charge.

In a second example, given the impedance measurement for a cell and its SOC during aging, we seek to predict a metric of its power fade. The MVLS net was trained using exemplars of two inputs—SOC and the total cell impedance measured at 100% SOC. Fig. 4 shows the surface generated by the trained MVLS network. Training data are also plotted as circles. The truncation in the ANN approximation indicates the end of the space where training data existed; therefore, only interpolation was performed. One potential use of this surface is to establish power degradation for states of charge not originally tested.

The final example is to use the ANN as a tool to validate an existing power fade model and to determine the limits of the space in which it is applicable with reasonable accuracy. A related use could be choosing the best model to represent a set of data from among several alternatives. For this example, we assume that a model, describing a particular cell behavior, exists (i.e. an Arrhenius-type model, an ANN model, etc.). Using experimental data, we can calculate the model prediction error, use an ANN to model this error, and develop an error prediction surface. This surface is

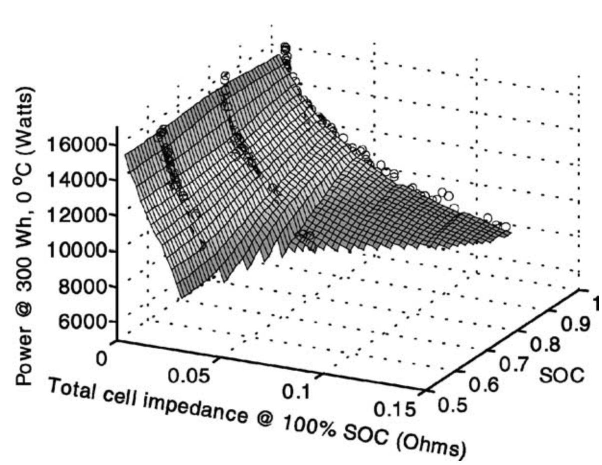

Fig. 4. ANN approximation of total cell impedance, SOC and power.

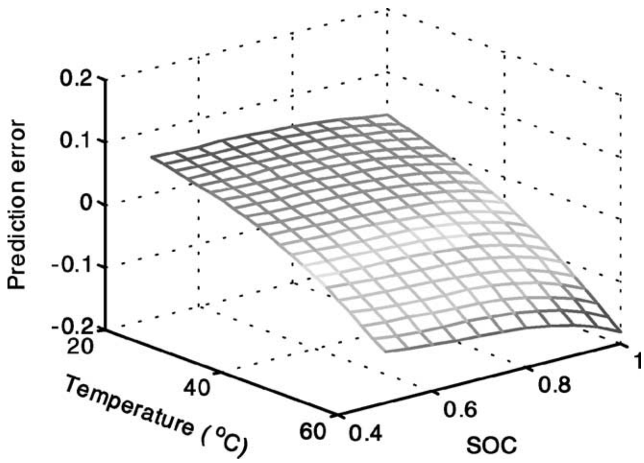

Fig. 5. ANN model of prediction error.

shown in Fig. 5. Using this plot, one could establish the limits of the applicability of the model by defining a level of accuracy (i.e. how much error is acceptable).

Our intent is to use this type of approach for cell life predictions under conditions of temperature and SOC that are within the range of experimental data. The model will also be capable of predicting cell performance at various stages of life under different conditions. These data reduction tools will continue to be applied to expand complex phenomena into separate components and to determine and interpret complex behavior mechanisms.

6. Summary

Aging experiments are being conducted on Li-ion cells as part of the ATD program. Power capability, capacity, and EIS measurements have been collected at 4-week intervals in order to develop a method to predict high-power battery life in HEV applications. Increasing interfacial impedance has been observed, which is correlated with decreasing cell power capability in a consistent way for each SOC tested. Inductive models of power fade have been shown to be capable of accurately representing power capability over the range of input parameters tested. These ANN models provide a capability to predict power fade at conditions that have not been tested, but that are within the range of the experimental parameters. It has also been shown that it is possible to use ANNs to describe and compare the prediction error surfaces for alternative life prediction models that could be applied to the aging data.

Acknowledgements

Sandia is a multiprogram laboratory operated by Sandia Corporation, a Lockheed Martin Company, for the United States Department of Energy, under contract DE-AC04-94AL85000. Support for this work was provided by the DOE Office of Advanced Automotive Technology through the Partnership for a New Generation of Vehicles (PNGV) Advanced Technology Development (ATD) High-Power Battery Program. The authors also wish to thank Carla Tatum and Bryan Sanchez for data processing.

References

[1] R.G. Jungst, et al., Meeting Abstracts, vol. 2001-2, Abstract No. 132, 200th ECS Mtg., San Francisco, CA, 2001.
[2] PNGV Battery Test Manual, DOE/ID-10597, Revision 3, 2001.
[3] R.G. Jungst, D.H. Doughty, B.Y. Liaw, G. Nagasubramanian, H.L. Case, E.V. Thomas, in: Proceedings of the 40th Power Sources Conference, Cherry Hill, NJ, 2002.
[4] (a) G. Nagasubramanian, J. Power Sources 87 (2000) 226;
(b) V. Manev, F. Kennard, M. Parsian, Abstract #358, 11th IMLB, Monterey, CA, 2002.
[5] R.D. Jones, et al., Nonlinear Adaptive Networks: A Little Theory, a Few Applications, Cognitive Modeling in System Control, The Santa Fe Institute.
[6] A. Urbina, et al., Characterization of Nonlinear Dynamic Systems Using Artificial Neural Networks, in: Proceedings of the 69th Shock and Vibration Symposium, Minneapolis, MN, 1998.